Quantum capacitance of double-layer graphene

Fariborz Parhizgar,[1] Alireza Qaiumzadeh,[2] and Reza Asgari[1,3,*]

[1]*School of Physics, Institute for Research in Fundamental Sciences (IPM), Tehran 19395-5531, Iran*

[2]*Department of Physics, Norwegian University of Science and Technology, NO-7491 Trondheim, Norway*

[3]*School of Nano Science, Institute for Research in Fundamental Sciences (IPM), Tehran 19395-5531, Iran*

(Received 7 May 2017; revised manuscript received 31 July 2017; published 31 August 2017)

We study the ground-state properties of a double-layer graphene system with the Coulomb interlayer electron-electron interaction modeled within the random-phase approximation. We first obtain an expression of the quantum capacitance of a two-layer system. In addition, we calculate the many-body exchange-correlation energy and quantum capacitance of the hybrid double-layer graphene system at zero temperature. We show an enhancement of the majority density layer thermodynamic density of states owing to an increasing interlayer interaction between two layers near the Dirac point. The quantum capacitance near the neutrality point behaves like a square root of the total density $\alpha\sqrt{n}$ where the coefficient α decreases by increasing the charge-density imbalance between two layers. Furthermore, we show that the quantum capacitance changes linearly by the gate voltage. Our results can be verified by current experiments.

DOI: 10.1103/PhysRevB.96.075447

I. INTRODUCTION

The conventional double layers based on semiconductors have amassed great interest for many years. Double-layer electron (hole) systems comprise two parallel quasi-two-dimensional (2D) electron (hole) layers in close proximity [1]. Such systems are useful structures to study various novel physical phenomena arising from the interlayer interaction effects specially at low particle densities or close proximity distance where many-body physics are significant. For instance, the observation of the fractional quantum Hall state at a half-filling factor which is forbidden in monolayer structures [2,3], the quantum Hall ferromagnetic phase transition [4], the Coulomb drag in a double-layer system [5], the quantum capacitance, and the electronic compressibility and transport properties of bilayer structures are systems where the interlayer interactions give rise to new physical properties.

Graphene, a flat sheet of carbon atoms arranged in a honeycomb lattice [6,7], after realization in 2004, has been attracting the attention of many scientists in different research areas from both technological and academic points of view. The low-energy charge carriers in pristine graphene behave as massless Dirac fermions. Since the density of states of monolayer graphene changes linearly as the Fermi energy, therefore, the quantum capacitance, which is a consequence of the Pauli principle [8] requires extra energy for filling a quantum system with electrons, can be changed by applying a gate voltage. The differential capacitance of graphene is linearly proportional to its electric potential when operated near the Dirac point. Recently, the local compressibility of graphene has been measured [9] and is consistent with the many-body calculations [10] of this quantity. Moreover, experiments [11] on measuring quantum capacitance in pristine graphene revealed the signature of many-body effects in agreement with theoretical calculations [12]. The quantum capacitance of graphene has been measured using a three-electrode electrochemical configuration [13], the graphene-insulator-semiconductor backgate [14], the metal-oxide-semiconductor structures [15], in double-layer capacitors [16], and the epitaxial graphene layers thermally elaborated on a carbon-terminated face [17]. The quantum capacitance of bilayer graphene has been measured [18] and studied theoretically [19] too. Furthermore, the ground-state properties and dynamical behavior of gapless and gapped graphene monolayers have been the subject of many theoretical studies [7,20,21].

Multilayer systems enhance the effects of interparticle interactions through the combination of reduced dimensionality and low particle density and by the layer index. In this article, we study the quantum capacitance of a double-layer graphene with imbalanced charge densities by using the screened Coulomb potentials within the random-phase approximation (RPA) to explore the effect of the interlayer interaction on the quantum capacitance. The exchange-correlation energy was investigated previously for a double quantum well [22] and double-layer graphene [23].

One of the main consequences of the electron-electron interaction in graphene is the enhancement of the renormalized Fermi velocity, especially at lower densities [24]. In contrast to massless Dirac fermions, the electron-electron interaction will result in the decreasing of the Fermi velocity in conventional 2D electron systems. We perform a theoretical study of the quantum capacitance and related quantities of a double-layer system. First of all, we generalize the expression of the quantum capacitance for a double-layer structure, and afterwards, by using the ground-state properties of the system, we numerically calculate the quantum capacitance. The determination of graphene quantum capacitance is of crucial interest because not only does it get access to the density of states directly, but also is an efficient way to explore various anomalies occurring near the Dirac point which might be difficult to probe only by transport measurement [1,11,25–27]. We show an enhancement of the majority density layer thermodynamic density of states owing to a reduction of the total electron density and thus an increasing interlayer interaction between two layers near the Dirac point. Our numerical results show that the quantum capacitance near the neutrality point behaves like a square root of the total

*asgari@ipm.ir

FIG. 1. Schematic of a double-layer system, including two graphene layers encapsulated by different materials and separated by a distance d from each other. The spacer distance is H, and the gate voltage is applied after the spacer material. The bias voltage and the charge-carrier densities together with corresponding voltages of each layer V_b, V_1, and V_2, respectively, are shown. Applying an electric-field E_2 on the top layer results in a penetrating field E_1 between layers. By connecting the bottom layer to a large resistance, the electric-field E_0 is fixed, and then the physical quantity $R_E = dE_1/dE_2$ can be obtained.

density $\alpha\sqrt{n}$ where the coefficient α decreases by increasing the charge-density imbalance between two layers. We also find that the quantum capacitance is sensitive to the bias voltage and depends on the gate voltage linearly, in contrast to a conventional 2D electron gas (2DEG) system where its quantum capacitance is independent of gate voltage.

This paper is organized as follows. In Sec. II we present our model, discuss the realization of our setup, and study the effect of the Coulomb interactions on the ground-state energy of the double-layer systems. We then discuss the quantum capacitance for the double-layer graphene systems. The numerical results and discussion are presented in Sec. III, and finally we conclude our results in Sec. IV with a summary and some remarks.

II. THEORY AND MODEL HAMILTONIAN

We consider a free-disordered double-layer structure incorporating a doped graphene layer (layer I) placed on another graphene layer (layer II) with a separation distance d at zero temperature. A schematic of the structure is shown in Fig. 1 where the electron densities in the layers are n_1 and n_2. We assume that each layer is about zero thickness in the direction normal to the plane of the system. The layers are separated by a dielectric material (shown in Fig. 1) with a dielectric constant ϵ_2, and we suppose that the tunneling of electrons between the layers is negligible, however, the Coulomb interlayer interaction plays an important role in the system. The effective Hamiltonian of the system under consideration reads

$$\hat{\mathcal{H}} = \sum_{\mathbf{k},l,\alpha,\beta} \hat{\psi}^{\dagger}_{\mathbf{k},l,\alpha} \hbar v_l \boldsymbol{\sigma}_{\alpha,\beta} \cdot \mathbf{k} \hat{\psi}_{\mathbf{k},l,\beta} + \frac{1}{2\mathcal{A}} \sum_{\mathbf{q}\neq 0,l,l'} \mathbf{V}_{ll'}(q) \hat{\rho}_{\mathbf{q},l} \hat{\rho}^{\dagger}_{\mathbf{q},l'}. \quad (1)$$

Here v_l is the Fermi velocity of layer $l = 1$ and 2, $\hat{\psi}_{\mathbf{k}}$'s are the corresponding two-component pseudospinors of the noninteracting Hamiltonian, $\mathcal{A}$ is the area of the system, $\mathbf{V}_{ll'}$ is the matrix of the bare Coulomb interactions, $\hat{\rho}_{\mathbf{q},l}$ is the density operator for the lth layer, α and β are the pseudospin indices, and $\boldsymbol{\sigma}$ is the Pauli matrix. In this Hamiltonian, the two layers are perfectly decoupled, and the long-range Coulomb interaction affects only the electrons in the layers. We define the retarded density-density linear-response functions $\chi_{ll'}(\mathbf{q},\omega) = \frac{1}{i\hbar}\lim_{\eta\to 0}\int_0^{\infty} e^{i(\omega+i\eta)t}\langle[\hat{\rho}_l(\mathbf{q},t),\hat{\rho}^{\dagger}_{l'}(\mathbf{q})]\rangle$, where η is an infinitesimal parameter and $\langle\cdots\rangle$ denotes the average in the thermal equilibrium ensemble. Note that, in our model, $\chi_{ll'} = \chi_l\delta_{l,l'}$. This quantity is related to several important many-body properties, such as the total ground-state energy, the electron compressibility, and the renormalized Fermi velocity [28]. Using the RPA, one can find $\chi^{-1}(\mathbf{q},\omega) = \chi^{(0)^{-1}}(\mathbf{q},\omega) - \mathbf{V}(q)$, where $\chi^{(0)}(\mathbf{q},\omega)$ is the noninteracting Lindhard matrix-response function of the Dirac fermions in the two-component systems. $V(q)$ is a 2×2 matrix including inter- and intralayer Coulomb interactions.

The intra- and interlayer Coulomb potentials are given by

$$V_{11}(q) = \frac{4\pi e^2}{qF(q)}[(\epsilon_2+\epsilon_3)e^{qd} + (\epsilon_2-\epsilon_3)e^{-qd}],$$
$$V_{12}(q) = V_{21}(q) = \frac{8\pi e^2}{qF(q)}\epsilon_2, \quad (2)$$

where $F(q) = (\epsilon_1+\epsilon_2)(\epsilon_2+\epsilon_3)e^{qd} + (\epsilon_1-\epsilon_2)(\epsilon_2-\epsilon_3)e^{-qd}$ and the interaction in the top layer can be obtained by replacing $\epsilon_1 \leftrightarrow \epsilon_3$ in $V_{11}(q)$. Here ϵ_i is the dielectric constant of the region ith.

The exchange and the correlation energies of a double-layer system in the RPA have been calculated in Ref. [23]. We follow that approach to calculate the ground-state energy of the system under consideration. We define the total Fermi wave vector of the system as $k_{\mathrm{F}} = \sqrt{4\pi n/g}$ $(n = n_1 + n_2)$ where $g(= g_s g_v)$ is the total spin (g_s) and valley (g_v) degeneracies.

Having calculated the ground-state energy, the electron compressibility and the quantum capacitance [8] can be obtained which are two important physical quantities to investigate many-body effects in 2D systems. These quantities are in fact related to the density of states.

The electron compressibility of a system [29] is related to the total energy as

$$\kappa^{-1} = n^2\frac{\partial\mu}{\partial n} = n^2\frac{\partial^2(n\varepsilon)}{\partial n^2}, \quad (3)$$

where μ is the chemical potential and the total energy per particle is $\varepsilon = \varepsilon_{\mathrm{kin}} + \varepsilon_x + \varepsilon_c$, where $\varepsilon_{\mathrm{kin}}$ is the total kinetic energy of the system: $\varepsilon_{\mathrm{kin}} = (g\varepsilon_{\mathrm{F}}/6)[\bar{k}^3_{\mathrm{F2}} + \bar{k}^3_{\mathrm{F1}}]$ where $k_{\mathrm{F}i} = \bar{k}_{\mathrm{F}i}k_{\mathrm{F}}$ denotes the Fermi wavelength of layer i and the energy quantities are scaled in units of $\varepsilon_{\mathrm{F}} = \hbar v_{\mathrm{F}}k_{\mathrm{F}}$. We assume that the density of states is symmetric with respect to the Fermi energy.

Eisenstein *et al.* [26] have introduced a powerful method to measure the compressibility of a 2DEG layer by locating another 2D layer in the proximity of the first layer. The spacer distance is H, and the gate voltage is applied after the spacer material (see Fig. 1). The bias voltage and the charge-carrier densities together with corresponding voltages of each layer V_b, V_1, and V_2 are considered, respectively. Applying an electric-field E_2 on the top layer results in a penetrating field E_1 between layers. By connecting the bottom layer to a large resistance, the electric-field E_0 is fixed, and

then the physical quantity $R_E = dE_1/dE_2$ can be measured. Before their experimental proposal, the measurement of the compressibility was based on measuring the capacitance between a 2DES layer and a metal gate. In this method, the capacitance was obtained by the sum of a large geometric contribution and a much smaller term $\partial\mu/\partial n$. It turns out that the first term made significant errors in the measurement. In the method of Eisenstein *et al.* [26], a double-quantum-well system was used as shown in Fig. 1. Using a large resistance connected to the bottom layer, one can fix the value of E_0. In addition, tuning the external field E_2 results in the field changes between layers E_1, and therefore, dE_1/dE_2 is the quantity which can be measured. Eisenstein *et al.* [26] used this method in a situation where the distance between layers was far enough so the interlayer correlations can be neglected and then measured the compressibility of the top layer. Jungwirth and MacDonald [27], on the other hand, extended their analysis for a narrow double-layer system where interlayer correlations play an important role.

The energy of the double-layer system in this configuration can be written up to an irrelevant constant by

$$\frac{E(n_1,n_2)}{\mathcal{A}} = \frac{e^2 d}{2\epsilon_2}(n_2 - n_0)^2 + n\varepsilon(n - n_2, n_2), \tag{4}$$

where the first term is the energy stored in a capacitor with two parallel metallic planes, n_2 and n_1 are the densities of the bottom and top layers, respectively, n_0 is a constant density, which is determined by E_0, and $\varepsilon(n_1,n_2)$ is the energy per particle of the double-layer system. From Poisson's equations and the electrostatic laws, we have

$$\epsilon_2 E_1 = \epsilon_3 E_0 - e n_2, \quad \epsilon_1 E_2 = \epsilon_3 E_0 - e(n_1 + n_2). \tag{5}$$

Changing E_2 varies the total density, whereas E_1 controls the electron-density n_2. Keeping in mind that E_0 is a constant value according to the large resistance and independent of the voltage, we thus define the Eisenstein ratio as $R_E = dE_1/dE_2 = (\epsilon_2/\epsilon_1)dn_2/dn$. Having given n, we can determine n_2 by minimizing the total energy using Eq. (4) with respect to n_2. We thus get the following equation $\mu_1 = \mu_2 + (e^2 d/\epsilon_2)(n_2 - n_0)$ where $\mu_i = \partial[n\varepsilon(n_1,n_2)]/\partial n_i$. Note that μ_i includes all contributions to the chemical potential for electrons in the ith layer except for contributions from the electrostatic potentials and would be the full chemical potential if neutralizing positive charges in each layer were assumed.

It follows from μ_i by taking the partial derivatives with respect to the density of the layers that

$$\frac{\partial\mu_1}{\partial n_1}dn_1 + \frac{\partial\mu_1}{\partial n_2}dn_2 = \frac{\partial\mu_2}{\partial n_1}dn_1 + \frac{\partial\mu_2}{\partial n_2}dn_2 + \frac{e^2 d}{\epsilon_2}dn_2, \tag{6}$$

and it turns out that

$$(d_{11} - d_{21})(dn - dn_2) = (d + d_{22} - d_{12})dn_2, \tag{7}$$

where we introduce a set of lengths as follows:

$$d_{ij} = \frac{\epsilon_2}{e^2}\frac{\partial\mu_i}{\partial n_j}, \tag{8}$$

where $i, j = 1, 2$ are layer labels. Accordingly, we find

$$\frac{dn_2}{dn} = \frac{d_{11} - d_{21}}{d + d_{11} + d_{22} - d_{21} - d_{12}}. \tag{9}$$

Note that, for the local minimum of the total energy per unit area, we require that the second derivative of the total energy Eq. (4) with respect to n_2 be positive. This gives a necessary condition for stability in which $d + d_{11} + d_{22} - d_{21} - d_{12} > 0$.

Moreover, the Eisenstein ratio [30] is defined by $R_E = \epsilon_2 C/\epsilon_1 C_1$ where $C_1 = \mathcal{A}e^2\partial n_1/\partial\mu_1$ and thus,

$$\frac{1}{C} = \frac{d_{11}}{\epsilon_2\mathcal{A}}\frac{d + d_{11} + d_{22} - d_{21} - d_{12}}{d_{11} - d_{21}}. \tag{10}$$

It is easy to decompose the above expression into two parts as

$$\frac{1}{C} = \frac{1}{\epsilon_2\mathcal{A}}\frac{d}{1 - \frac{d_{21}}{d_{11}}} + \frac{1}{\epsilon_1\mathcal{A}}\frac{d_{11} + d_{22} - d_{21} - d_{12}}{1 - \frac{d_{21}}{d_{11}}}. \tag{11}$$

Since $d_{21} \ll d_{11}$, we can approximate the denominator by unity, and thus the capacitance C, which contains two contributions in the series, is

$$\frac{1}{C} = \frac{1}{C_g} + \frac{1}{C_Q}, \tag{12}$$

where $C_g = \mathcal{A}\epsilon_2/d$ is the geometrical capacitance and the quantum capacitance can be defined as

$$C_Q = \mathcal{A}\frac{e^2}{\partial\mu_1/\partial n_1 + \partial\mu_2/\partial n_2 - \partial\mu_1/\partial n_2 - \partial\mu_2/\partial n_1}. \tag{13}$$

This expression of the quantum capacitance is a main equation in this paper. In the classical limit where $\hbar \to 0$ and $m \to \infty$ one finds $C_Q \to \infty$ and finally $C = C_g$. However, in the quantum regime, one can expect interesting effects when C_Q becomes compatible to the geometrical capacitance. Furthermore, by considering $d \to \infty$, this expression reduces to the well-known expression of the monolayer quantum capacitance where $C_Q = \mathcal{A}e^2\frac{\partial n_2}{\partial\mu_2}$.

III. NUMERICAL RESULTS

In this section, we present our numerical results of the quantum capacitance using the ground-state energy at zero temperature through Eqs. (8)–(13). Here we introduce a density asymmetry parameter between two layers $-1 < \xi = (n_2 - n_1)/n < 1$.

Exchange and correlation energies in the system depend both on interactions on the Fermi wavelength scale which influence correlations between carriers and on interactions at shorter length scales which influence correlation with the Dirac sea background [23]. Because decoupled graphene layers are separated by atomic length scales and carrier densities are always small, thus the atomic scale $k_{F,l}d$ is typically small. Here, the exchange energies are positive [23] because they are calculated relative to zero carrier density using the Dirac point self-energy of this limit as the zero of energy and owing to its chirality. The increase in the exchange energy with the carrier density in graphene has the physical consequence of an enhancement of the screening and therefore, increasing the renormalized Fermi velocity instead of weakening it as in an ordinary 2D electron gas. The correlation energy, which is negative, is dramatically higher in the decoupled graphene

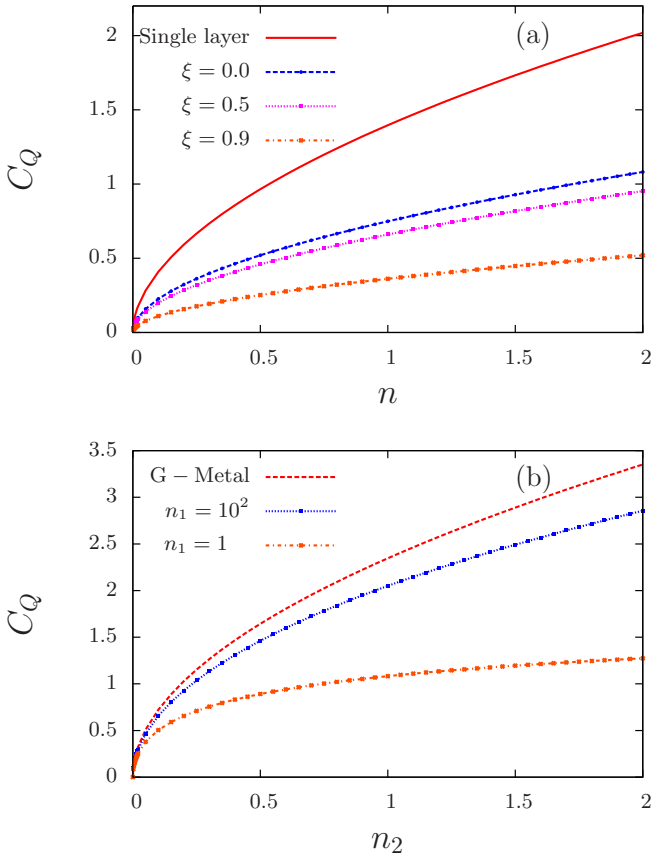

FIG. 2. (a) The quantum capacitance (in units of μF cm^{-2}) from Eq. (13) as a function of the electron-density $n = n_1 + n_2$ (in units of 10^{12} cm^{-2}) for different values of the density imbalance $\xi = (n_2 - n_1)/n$. Here we consider $d = 1$ nm, $\epsilon_1 = 1$ with H tends to infinity, $\epsilon_2 = 4.5$, and $\epsilon_3 = 4.5$. The solid curve shows the quantum capacitance of single-layer graphene. (b) The quantum capacitance (in units of μF cm^{-2}) as a function of the electron-density n_2 (in units of 10^{12} cm^{-2}) for different n_1 values (in units of 10^{12} cm^{-2}) in comparison with that in a system incorporates encapsulated graphene with hexagonal boron nitride and placed by a metal at a distance of $d = 1$ nm studied in Ref. [12].

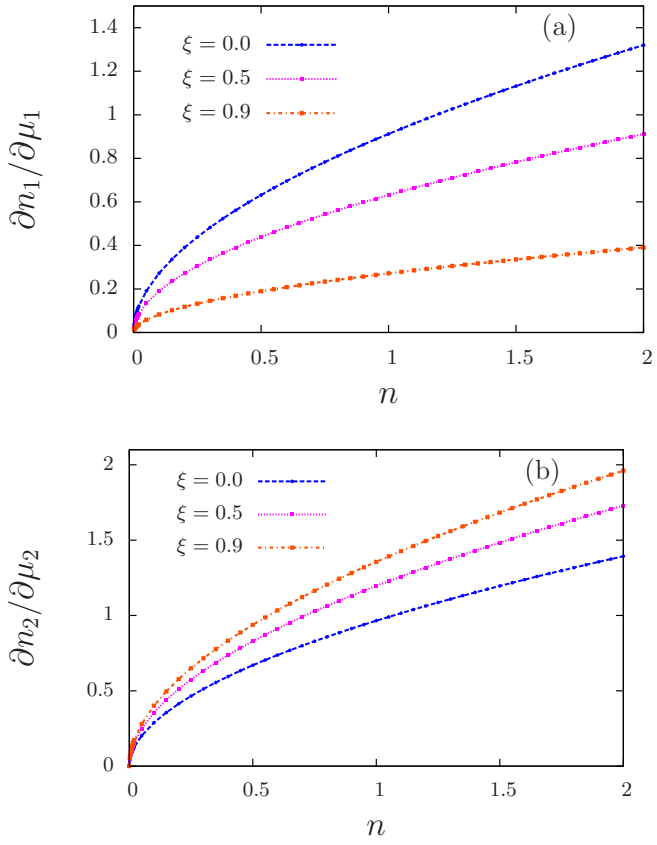

FIG. 3. The thermodynamic density-of-states $\partial n_i/\partial \mu_i$ [in units of 10^{10}/(meV cm^2)] where $i = 1$ or 2 as a function of the electron-density $n = n_1 + n_2$ (in units of 10^{12} cm^{-2}) for different values of the density imbalance. We consider $d = 1$ nm, $\epsilon_1 = 1$ with H tends to infinity, $\epsilon_2 = 4.5$, and $\epsilon_3 = 4.5$.

layer in comparison to that in monolayer graphene, strongly influenced by interlayer interactions, and resulting in the increased quantum capacitance.

Having calculated the ground-state energies based on the method reported in Ref. [23], we can calculate some interesting transport properties. The quantum capacitance as a function of the total electron density on the two layers is presented in Fig. 2(a). The quantum capacitance starts from zero in clean systems at the Dirac point and increases by increasing the electron density owing to the fact that the renormalized Fermi velocity decreases. The behavior of C_Q near the neutrality point is no longer linear and can be fitted quite well with the total density as $\alpha\sqrt{n}$ where the coefficient α decreases by increasing the density imbalance ξ. These are happening owing to the change in the Fermi velocity stemming from the increasing of the Coulomb interlayer interaction [23]. Our numerical results show that the quantum capacitance is suppressed by increasing the charge imbalance between two layers. We also calculate a quantum capacitance of a monolayer layer system (the same as in Fig. 1 when $d \to \infty$), and the result is shown in Fig. 2(a) as a solid line. In order to perceive the role of the Coulomb interactions, we compare the results with that in a system when a metal gate exists on the top of the encapsulated monolayer graphene [12]. The quantum capacitance as a function of the electron-density n_2 for different n_1's is illustrated in Fig. 2(b). First of all, there is an enhancement of the quantum capacitance when a metal is located close to the system. Furthermore, by reducing n_1, $\partial\mu_1/\partial n_1$ increases, and thus C_Q decreases. Therefore, by increasing n_1, the quantum capacitance of the double-layer graphene approaches the quantum capacitance of a graphene system in the presence of the metal gate.

The thermodynamic density-of-states $\partial n_i/\partial \mu_i$ for layer $i = 1, 2$ as a function of the total electron-density n are shown in Fig. 3. The thermodynamic density of states decreases with increasing ξ for layer I with the minority electron-density $n_1 = n(1 - \xi)/2$, $\partial n_2/\partial \mu_2$ increases, therefore, the interlayer interaction contribution of the minority density is dominated and results in increasing the thermodynamic density of states in the second layer. In the absence of interlayer interactions, $d_{12} = d_{21} = 0$, and thus d_{ii} is related directly to the electronic compressibility in layer i.

In Fig. 4, we demonstrate the Eisenstein ratio dn_2/dn as a function of the total density n. The advantage of measuring

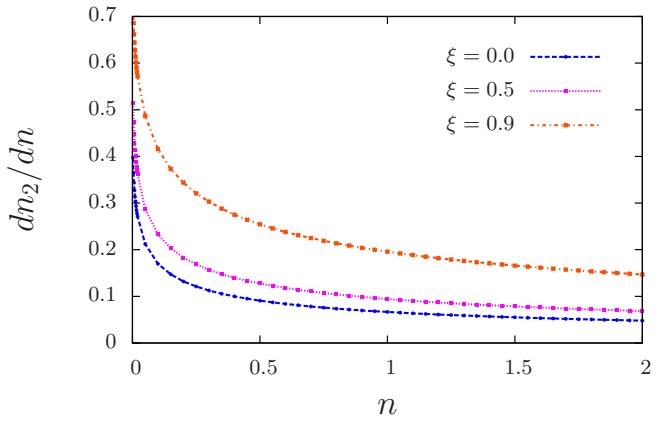

FIG. 4. The Eisenstein ratio dn_2/dn from Eq. (9) as a function of the electron-density $n = n_1 + n_2$ (in units of 10^{12} cm^{-2}) for different values of the density imbalance and $d = 1$ nm, $\epsilon_1 = 1$ with H tends to infinity, $\epsilon_2 = 4.5$, and $\epsilon_3 = 4.5$.

dn_2/dn is that this quantity depends only on the electronic lengths d_{ij} and the interlayer distance d. By increasing the electron-density imbalance, d_{11} increases as well as R_E.

Finally, in order to connect this study to an experimental setup, we change the charge-carrier densities or the top and bottom chemical potentials μ_1 and μ_2, respectively, to the gate voltage V_G and the interlayer bias V_b assuming that all quantities are uniform in the horizontal directions [23,31]. The bias voltage can be defined by the difference between the electrochemical potentials of the top and bottom layers and reads as

$$V_b = V_1 - V_2 - (\mu_1 - \mu_2)/e. \tag{14}$$

Another electrostatic relation follows from the charge neutrality condition where $n_1 + n_2 + n_G = 0$ where n_G is the electron-density associated with the gate voltage. These carrier densities are related to the electric fields (in what follows, we set $n_0 = 0$, and it means that all electric fields are measured with E_0),

$$E_2 = -en_G/\epsilon_1, \quad \epsilon_2 E_1 = \epsilon_1 E_2 - en_1. \tag{15}$$

Furthermore, the electric fields are connected to the voltages on the graphene layers and on the gate by

$$E_2 = -(V_1 - V_G)/H, \quad E_1 = -(V_2 - V_1)/d, \tag{16}$$

and the chemical potential for each layer can be calculated through $\mu_i = \partial[n\varepsilon(n_1,n_2)]/\partial n_i$ where $\varepsilon(n_1,n_2)$ is the ground-state energy per particle of the system calculated through the RPA. These aforementioned sets of equations can be solved for unknown μ_1, μ_2, E_1, E_2, V_1, V_2, and V_G for given n_1 and n_2 values.

In Fig. 5(a) we plot the quantum capacitance in units of μF cm^{-2} as functions of the charge-carrier densities n_1 and n_2 in units of 10^{12} cm^{-2} for $d = 3.5$ and $H = 30$ nm when graphene layers are encapsulated by hexagonal boron nitride. C_Q increases noticeably with increasing layer densities. Furthermore, C_Q is demonstrated as functions of the top gate V_1 and bias potential V_b which is given by Eq. (14) in Fig. 5(b). The domain of the potentials is considered in small regions. We find that the quantum capacitance is sensitive to both potentials

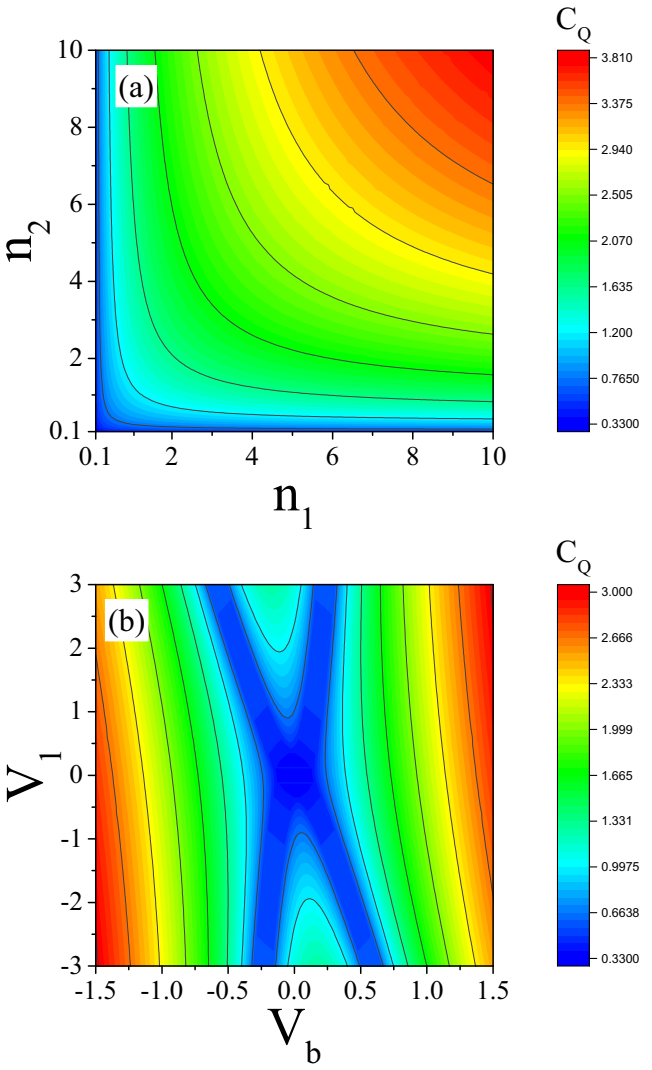

FIG. 5. The quantum capacitance (in units of μF cm^{-2}) as functions of (a) the electron-densities n_1 and n_2 (in units of 10^{12} cm^{-2}) and (b) the top gate and bias potential in units of eV for $d = 3.5$ and $H = 30$ nm when graphene layers are encapsulated by hexagonal boron nitride where $\epsilon_i = 4.5$ for $i = 1$–3. Notice that since H/d is very large, the formalisms given by Eqs. (1) and (2) are valid.

and it depends on the gate voltage linearly, in contrast to a conventional 2D electron gas system where its quantum capacitance is independent of gate voltage. We stress that the implications of the findings reported in this paper are applicable to any graphene device that involves a metal-graphene contact. For example, for a graphene-based field-effect transistor, it has widely been reported that the contact resistance between the metal and the graphene exhibits an asymmetry with respect to the polarity of the gate potential [9,32].

IV. SUMMARY AND CONCLUSION

In conclusion, we have presented a theoretical scheme, based on the random-phase approximation, to investigate the effects of Coulomb interactions on observable quantities of decoupled graphene Fermi-liquid systems encapsulated by dielectric materials, such as the quantum capacitance and charge

compressibility. We have carried out microscopic calculations to explore the ground-state properties of the system with the Coulomb interlayer electron-electron interaction modeled within the random-phase approximation. Importantly, an expression for describing the quantum capacitance for a two-layer system is derived. We have shown that the quantum capacitance near the neutrality point can be well behaved by $\alpha\sqrt{n}$ (linear behavior to the gate voltage) where the prefactor α decreases by increasing the charge-density imbalance between two layers. An enhancement of the majority density layer thermodynamic density of states due to a reduction of the total electron density is calculated. We have also shown that the quantum capacitance increases by locating a metal on top of the considered system. Furthermore, we have found that the quantum capacitance is sensitive to the top and bottom potentials and the gate voltage dependence on the quantum capacitance is linear, in contrast to a conventional 2D electron gas system where its quantum capacitance is independent of gate voltage.

ACKNOWLEDGMENTS

We would like to thank K. Novoselov and M. Polini for fruitful discussions. This work was partially supported by Iran Science Elites Federation Grant No. 11/66332.

[1] L. Świerkowski, D. Neilson, and J. Szymański, Aust. J. Phys. **46**, 423 (1993); B. Tanatar and B. Davoudi, Phys. Rev. B **63**, 165328 (2001).

[2] G. S. Boebinger, H. W. Jiang, L. N. Pfeiffer, and K. W. West, Phys. Rev. Lett. **64**, 1793 (1990); A. H. MacDonald, P. M. Platzman, and G. S. Boebinger, *ibid.* **65**, 775 (1990); Y. W. Suen, J. Jo, M. B. Santos, L. W. Engel, S. W. Hwang, and M. Shayegan, Phys. Rev. B **44**, 5947 (1991); S. Q. Murphy, J. P. Eisenstein, G. S. Boebinger, L. N. Pfeiffer, and K. W. West, Phys. Rev. Lett. **72**, 728 (1994).

[3] Y. W. Suen, L. W. Engel, M. B. Santos, M. Shayegan, and D. C. Tsui, Phys. Rev. Lett. **68**, 1379 (1992); J. P. Eisenstein, G. S. Boebinger, L. N. Pfeiffer, K. W. West, and S. He, *ibid.* **68**, 1383 (1992).

[4] K. Yang, K. Moon, L. Zheng, A. H. MacDonald, S. M. Girvin, D. Yoshioka, and S.-C. Zhang, Phys. Rev. Lett. **72**, 732 (1994).

[5] T. J. Gramila, J. P. Eisenstein, A. H. MacDonald, L. N. Pfeiffer, and K. W. West, Phys. Rev. Lett. **66**, 1216 (1991); R. V. Gorbachev, A. K. Geim, M. I. Katsnelson, K. S. Novoselov, T. Tudorovskiy, I. V. Grigorieva, A. H. MacDonald, S. V. Morozov, K. Watanabe, T. Taniguchi, and L. A. Ponomarenko, Nat. Phys. **8**, 896 (2012).

[6] K. S. Novoselov, A. K. Geim, S. V. Morozov, D. Jiang, Y. Zhang, S. V. Dubonos, I. V. Grigorieva, and A. A. Firsov, Science **306**, 666 (2004).

[7] A. H. Castro Neto, F. Guinea, N. M. R. Peres, K. S. Novoselov, and A. K. Geim, Rev. Mod. Phys. **81**, 109 (2009).

[8] S. Luryi, Appl. Phys. Lett. **52**, 501 (1988).

[9] J. Martin, N. Akerman, G. Ulbricht, T. Lohmann, J. H. Smet, K. von Klitzing, and A. Yacoby, Nat. Phys. **4**, 144 (2008).

[10] R. Asgari, M. M. Vazifeh, M. R. Ramezanali, E. Davoudi, and B. Tanatar, Phys. Rev. B **77**, 125432 (2008); N. M. R. Peres, F. Guinea, and A. H. Castro Neto, *ibid.* **72**, 174406 (2005); E. H. Hwang, Ben Yu-Kuang Hu, and S. Das Sarma, Phys. Rev. Lett. **99**, 226801 (2007); D. E. Sheehy and J. Schmalian, *ibid.* **99**, 226803 (2007).

[11] G. L. Yu, R. Jalil, B. Belle, A. S. Mayorov, P. Blake, F. Schedin, S. V. Morozov, L. A. Ponomarenko, F. Chiappini, S. Wiedmann, U. Zeitler, M. I. Katsnelson, A. K. Geim, K. S. Novoselov, and D. C. Elias, Proc. Natl. Acad. Sci. USA **110**, 3282 (2013).

[12] R. Asgari, M. I. Katsnelson, and M. Polini, Ann. Phys. (Berlin) **526**, 359 (2014); Y. E. Lozovik, A. A. Sokolik, and A. D. Zabolotskiy, Phys. Rev. B **91**, 075416 (2015).

[13] J. Xia, F. Chen, J. Li, and N. Tao, Nat. Nanotechnol. **4**, 505 (2009).

[14] F. Giannazzo, S. Sonde, V. Raineri, and E. Rimini, Nano Lett. **9**, 23 (2009).

[15] H. Xu, Z. Zhang, and L.-M. Penga, Appl. Phys. Lett. **98**, 133122 (2011).

[16] H. Ji, X. Zhao, Z. Qiao, J. Jung, Y. Zhu, Y. Lu, L. L. Zhang, A. H. MacDonald, and R. S. Ruoff, Nat. Commun. **5**, 3317 (2014).

[17] A. B. Trabelsi, F. V. Kusmartsev, D. M. Forrester, O. E. Kumartseva, M. B. Gaifullin, P. Cropper, and M. Oueslati, J. Mater. Chem. C **4**, 5829 (2016).

[18] E. A. Henriksen and J. P. Eisenstein, Phys. Rev. B **82**, 041412 (2010); C. Liu and J.-L. Zhu, Phys. Lett. A **377**, 2966 (2013); K. Nagashio, K. Kanayama, T. Nishimura, and A. Toriumi, ECS Trans. **61**, 75 (2014).

[19] G. S. Kliros, Rom. J. Inform. Sci. Tech. **13**, 332 (2010); A. F. Young and L. S. Levitov, Phys. Rev. B **84**, 085441 (2011).

[20] A. Qaiumzadeh, F. K. Joibari, and R. Asgari, Eur. Phys. J. B **74**, 479 (2010); A. Qaiumzadeh and R. Asgari, Phys. Rev. B **79**, 075414 (2009); New J. Phys. **11**, 095023 (2009).

[21] P. K. Pyatkovskiy, J. Phys.: Condens. Matter **21**, 025506 (2009).

[22] L. Zheng and A. H. MacDonald, Phys. Rev. B **49**, 5522 (1994).

[23] R. E. V. Profumo, M. Polini, R. Asgari, R. Fazio, and A. H. MacDonald, Phys. Rev. B **82**, 085443 (2010).

[24] M. Polini, R. Asgari, Y. Barlas, T. Pereg-Barnea, and A. H. MacDonald, Solid State Commun. **143**, 58 (2007); G. Borghi, M. Polini, R. Asgari, and A. H. MacDonald, *ibid.* **149**, 1117 (2009).

[25] G. F. Giuliani and G. Vignale, *Quantum Theory of the Electron Liquid* (Cambridge University Press, Cambridge, UK, 2005).

[26] J. P. Eisenstein, L. N. Pfeiffer, and K. W. West, Phys. Rev. Lett. **68**, 674 (1992); Phys. Rev. B **50**, 1760 (1994).

[27] T. Jungwirth and A. H. MacDonald, Phys. Rev. B **53**, 9943 (1996).

[28] Y. Barlas, T. Pereg-Barnea, M. Polini, R. Asgari, and A. H. MacDonald, Phys. Rev. Lett. **98**, 236601 (2007).

[29] G. Borghi, M. Polini, R. Asgari, and A. H. MacDonald, Phys. Rev. B **82**, 155403 (2010).

[30] C. B. Hanna, D. Haas, and J. C. Díaz-Vélez, Phys. Rev. B **61**, 13882 (2000); J. C. Díaz-Vélez, *Meeting of the American Physical Society, Austin, TX, 2003* (APS, Ridge, NY, 2003).

[31] K. A. Guerrero-Becerra, A. Tomadin, and M. Polini, Phys. Rev. B **93**, 125417 (2016).

[32] F. Xia, V. Perebeinos, Y.-M. Lin, Y. Wu, and P. Avouris, Nat. Nanotechnol. **6**, 179 (2011); M.-Y. Lin, Y.-H. Chen, C.-F. Su, S.-W. Chang, S.-C. Lee, and S.-Y. Lin, Appl. Phys. Lett. **104**, 023511 (2014).